Soft Matter

Dynamic Article Links

Cite this: *Soft Matter*, 2012, **8**, 3062

www.rsc.org/softmatter

COMMUNICATION

Doubly crosslinked hydrogels prepared from pH-responsive vinyl-functionalised hollow particle dispersions†

Robert Bird,[a] Somjit Tungchaiwattana,[a] Tony Freemont[b] and Brian R. Saunders*[a]

Received 13th December 2011, Accepted 2nd February 2012
DOI: 10.1039/c2sm07366h

Vinyl-functionalised pH-responsive hollow particles have been prepared for the first time and used to construct physical and doubly crosslinked (DX) hydrogels. The pH-responsive DX hydrogels do not redisperse, have a high storage modulus with interconnected porosity and should be useful for regenerative medicine applications.

Hollow particles continue to intrigue researchers[1–7] and have a number of potential applications including intracellular delivery,[3] drug delivery[4,8,9] and feedback active coatings.[10] Recently, hollow particles have shown good promise for cartilage regeneration.[11] Although the hollow particles provided a beneficial morphology,[11] the dispersions did not form gels and would have limited potential to support load immediately after injection. Injectable gels that support load and also possess high internal porosity have excellent potential for regenerative medicine applications. Hydrogels are widely studied in the context of tissue engineering.[12,13] Unfortunately, it is difficult to control their porosity and its interconnectivity at the micrometre length scale. Recently, we showed that physical gels can be prepared using pH-responsive hollow particles.[14,15] The particle shells were crosslinked using reversible disulfides bonds. The physical gels were not permanent (no covalent interlinkages between particles) and redispersed if placed in water. This severely limits their potential applications. One possible method to achieve durable hydrogels is to covalently interlink swollen microgel particles.[16] However, those systems lacked interconnected porosity, which is essential for many regenerative medicine applications. In the present study we show for the first time that vinyl-functionalised pH-responsive hollow particles can be covalently interlinked to give injectable pH-responsive hydrogels with interconnected micrometre-scale porosity.

The starting point for our new hydrogels is collapsed hollow particle dispersions of non-crosslinked poly(MMA-*co*-MAA). MMA and MAA are methylmethacrylate and methacrylic acid. The dispersion was prepared using a method established earlier[15]—see Scheme S1 (ESI†). The number-average molecular weight and polydispersity for poly(MMA-*co*-MAA) were 27 300 g mol^{-1} and 1.9. The hollow particles form because the amphiphilic copolymer phase separates at the CH_2Cl_2/water interface.[14,15] The poly(MMA-*co*-MAA) particles dissolve when the pH is increased to the pK_a unless the shells are crosslinked.[15] Previously, we used cystamine for that purpose. Here, we functionalised the particles with aminoethyl methacrylate (AEM) and prepared the first examples of pH-responsive hollow particles crosslinked with vinyl groups, *i.e.*, poly(MMA-*co*-MAA)/AEM particles (Step 1, Scheme 1). Vinyl functional groups provide a more robust source of crosslinking (*cf.* cystamine[15]). (The methods used here are described in the ESI†.) The crosslinking first occurred within the shells (intra-shell crosslinking) and these particles are termed singly crosslinked (SX) particles. The SX particles were functionalised with AEM for a second time to give poly(MMA-*co*-MAA)/AEM(2) which enabled subsequent formation of doubly crosslinked (DX) gels (Step 2, Scheme 1) by photocrosslinking of unreacted AEM groups within a pH-triggered physical gel. This was possible because the poly(MMA-*co*-MAA) particles contained enough MAA to enable functionalisation for two crosslinking steps, whilst leaving sufficient unreacted MAA groups to give pH-triggered dispersion gelation. The DX gels were prepared by covalent linking of neighbouring AEM groups from inter-penetrating hollow particle shells. This new method converts a space-filling gel into a covalently-linked gel. Because the key requirement for the copolymers used in this approach is that they

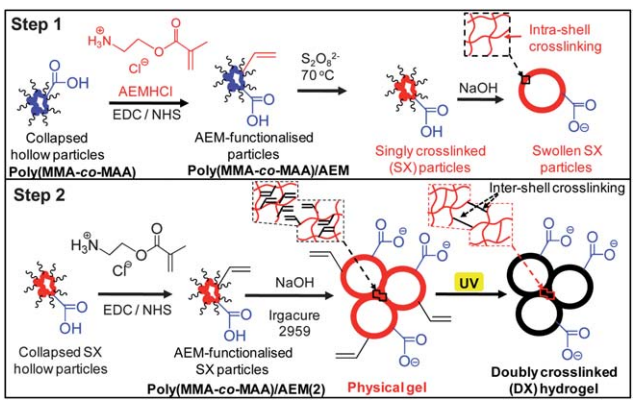

Scheme 1 Preparation of doubly crosslinked (DX) hydrogels from pH-responsive hollow particles. The SX poly(MMA-*co*-MAA)/AEM particles (Step 1) have intra-shell crosslinking. The DX hydrogel (Step 2) has both intra-shell and inter-shell crosslinking.

[a]*Biomaterials Research Group, School of Materials, The University of Manchester, Grosvenor Street, Manchester, M1 7HS, UK. E-mail: brian.saunders@manchester.ac.uk*
[b]*Tissue Injury and Repair Group, School of Medicine, Stopford Building, The University of Manchester, Oxford Road, Manchester, M13 9PT, UK*
† Electronic Supplementary Information (ESI) available. See DOI: 10.1039/c2ra07366h/

contain a hydrophobic segment and RCOOH segments, we believe the approach introduced here should be applicable to a large range of copolymers. A key advantage of our approach is that a colloidal template (*e.g.*, silica[4,17]) is not required to prepare the hollow particles. The methods used to prepare the pH-responsive hollow particles and DX hydrogel (Scheme 1) are scaleable.

The poly(MMA-*co*-MAA), poly(MMA-*co*-MAA)/AEM and poly(MMA-*co*-MAA)/AEM(2) particles (Scheme 1) were characterised by titration (Fig. S1, ESI†). The apparent pK_a of the poly-(MMA-*co*-MAA) particles was 6.4 and they contained 43 mol.% MAA. The pK_a increased with decreasing MAA content (Fig. S1(b), ESI†). SX poly(MMA-*co*-MAA)/AEM hollow particles contained 26 mol.% MAA. The maximum extent of AEM functionalisation was 17 mol.%. The SX particles functionalised for a second time (poly(MMA-*co*-MAA)/AEM(2)) contained 18 mol.% MAA, giving a maximum AEM functionalisation for this step of 8 mol.% The actual values may be lower because competing reactions can occur during EDC coupling reactions.[18] ^{1}H NMR spectra for poly(MMA-*co*-MAA) and poly(MMA-*co*-MAA)/AEM are shown in Fig. S2 (ESI†). Small peaks due to vinyl groups were present in the spectra for poly(MMA-*co*-MAA)/AEM (Fig. S2(b), ESI†). Although these data show that functionalisation was successful, the intensity was low because the copolymer did not fully dissolve which broadened the peaks.

Fig. 1(a) shows an optical micrograph of the new SX poly(MMA-*co*-MAA)/AEM hollow particles. They were collapsed at pH = 6. They are polydisperse because of the emulsion-based method for preparation (ESI†). If required, the polydispersity could be reduced using fractionation. An SEM image of the SX hollow particles (Fig. 1(b)) shows that they have collapsed substantially on drying in the high vacuum of the SEM instrument. The hollow particles folded inwards upon themselves, which is apparent from the inset of Fig. 1(b). A representative TEM image (Fig. 1(c)) reveals that the shells appear to consist of overlapping small nanoparticles. The particles swelled rapidly when the pH of the dispersion increased (Fig. 1(d)). This is due to their relatively thin shell.

Fig. 1(e) shows the pH dependence of the volume swelling ratio for the SX poly(MMA-*co*-MAA)/AEM particles. The particles swelled strongly when the pH exceeded 7.3. The swelling ratio reached about 8 at pH = 9. The pH-triggered swelling behaviour of the particles is similar to those of cystamine-crosslinked poly(MMA-*co*-MAA) particles.[15] However, for the AEM-crosslinked particles the onset swelling pH (about 7.3) coincides with physiological pH (7.4) which may provide improved potential for triggered release *in vivo*.

Strong physical gels formed from the SX poly(MMA-*co*-MAA)/AEM hollow particle dispersions at concentrations greater than 5 wt.% when the pH reached 7.7 (See Fig. 2(a)). This is due to the effective volume fraction occupied by the swollen particles exceeding that available for relative particle movement. The particles become sterically confined and can interpenetrate. Gels were present at

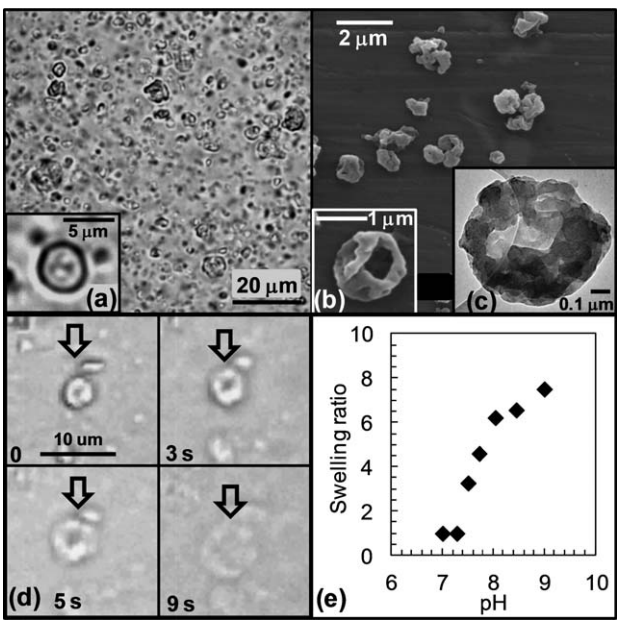

Fig. 1 SX poly(MMA-*co*-MAA)/AEM hollow particles (a) Optical micrograph of dispersed particles at pH of 6. (b) SEM image of hollow particles deposited at pH of 6. (c) shows a TEM image of a particle deposited at pH = 6. (d) optical micrograph of a collapsed hollow particle when a pH = 8.4 buffer front caused it to swell. The arrows show the particle. (e) Volume swelling ratio of particles as a function of pH.

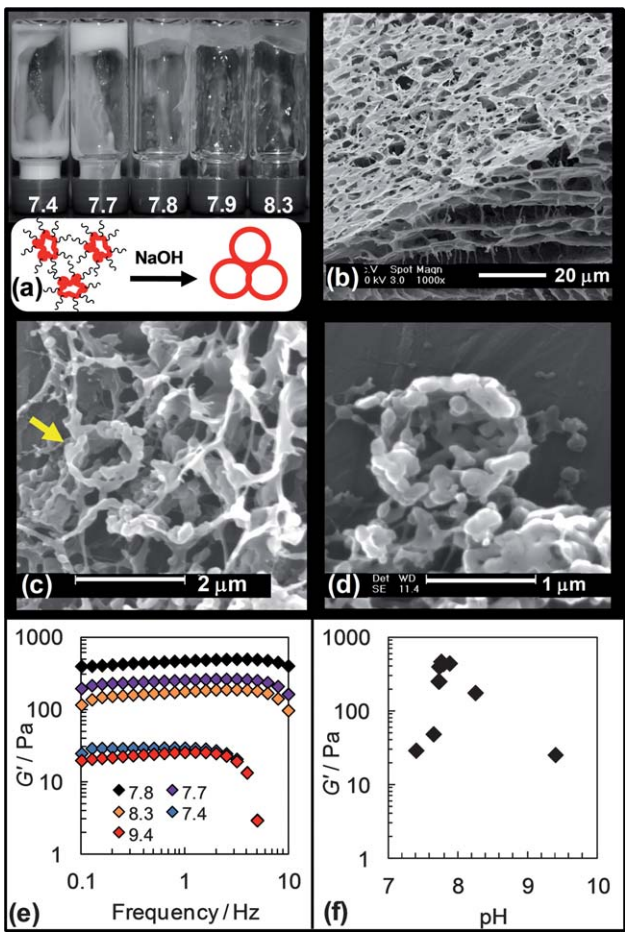

Fig. 2 Physically gelled SX poly(MMA-*co*-MAA)/AEM hollow particle dispersions (a) Digital photographs of dispersions at different pH values. (b) and (c) show SEM images of freeze-dried gels. The arrow in (c) highlights a hollow particle fragment. (d) Shows an individual hollow particle that has fragmented. The pH was 8.1 (b) or 7.7 ((c) and (d)). (e) shows frequency sweep data for particle dispersions at different pH values (shown). (f) shows the variation of G' with pH for physical gels (1 Hz). The particle concentrations were 5 wt%.

pH = 7.4 but were too weak (at 5 wt%) to support their own weight (Fig. 2(a)). It should be noted that the gel strength (elasticity) can be increased using higher particle concentrations. All of the gel data presented here were obtained using a particle concentration of 5 wt.%.

SEM images of a freeze-dried poly(MMA-*co*-MAA)/AEM physical gel are shown in Fig. 2(b) and (c). These images show interconnected porosity which permeates the gels. Interconnected porosity was observed earlier for physical gels prepared using cystamine-crosslinked hollow particles.[15] The fact that this morphology is evident for the SX poly(MMA-*co*-MAA)/AEM gels shows that it is a general feature of these new gel-forming dispersions and is not determined by the crosslinking monomer used. We noticed occasional single hollow particles that appeared to be fragmented, both within the gel (yellow arrow in Fig. 2(c)) and isolated from the gel samples during the freeze-drying process. Fig. 2(d) shows an SEM image of one such particle. The nanoparticulate nature of this shell is evident. More uniform shells also occurred (see Fig. S3, ESI†); however, even they were not fully intact. We propose that differences in shell morphology (nanoparticulate *vs.* uniform) originate in local shear variations during initial hollow particle formation. These SEM images suggest that the interconnected porosity (Fig. 2(b) and (c)) is due to (partial) particle fragmentation. The mechanism by which these morphologies occur is discussed below. An interconnected porous morphology is a desirable feature for tissue scaffolds[1] because it permits good nutrient supply within a 3D environment and the possibility of extracellular matrix ingrowth.

Fig. 2(e) shows frequency sweep data for the physically gelled SX poly(MMA-*co*-MAA)/AEM dispersions obtained at different pH values. The frequency dependence of G' (storage modulus) was low. The tanδ data (Fig. S4(a), ESI†) showed extended frequency independence at pH = 7.8. (Note that $\tan\delta = G''/G'$, where G'' is the loss modulus.) This indicates that this gel has the most ideal elastic response[19,20] of all the gels studied. This pH also corresponds to the maximum G' (Fig. 2(f)) and minimum tanδ value (Fig. S4(b), ESI†), which further shows that the elasticity of the gel was close to optimum at this pH. At higher pH values G' decreased and tanδ increased (Fig. S4(b), ESI†). The decrease of G' indicates a decreased number density of elastically effective chains. This is most like due to electrostatic screening from added NaOH. High electrolyte concentrations reduce hollow particle swelling and decrease inter-shell interpenetration.

The SX poly(MMA-*co*-MAA)/AEM particles were functionalised with AEM for a second time (Step 2, Scheme 1) to give poly(MMA-*co*-MAA)/AEM(2) and enable inter-shell crosslinking from the physically gelled state. These AEM-functionalised SX particles had the same folded morphology when viewed using SEM (Fig. S5(a), ESI†) as the precursor poly(MMA-*co*-MAA)/AEM particles (Fig. 1(b)). The poly(MMA-*co*-MAA)/AEM(2) particles formed physical gels with interconnected porosity (Fig. S5(b), ESI†). The pH chosen (8.1) for UV photocrosslinking (Step 2, Scheme 1) provided gels with low turbidity which gave improved efficiency of photocrosslinking during DX gel preparation as judged by the mechanical properties.

Whereas physically gelled dispersions have reversible interparticle bonds, a covalently-linked particle gel should have irreversible interparticle bonds. To assess this we tested the ability to redisperse the DX hydrogels (Fig. 3(a)). The dissolution tests showed that a control SX poly(MMA-*co*-MAA)/AEM physical gel redispersed.

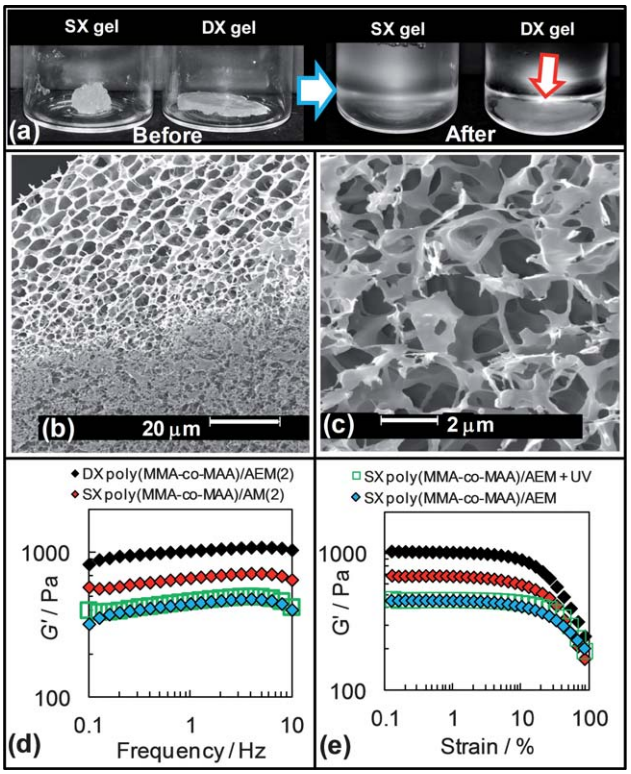

Fig. 3 DX hydrogels from poly(MMA-*co*-MAA)/AEM(2) hollow particles (a) shows a physical SX poly(MMA-*co*-MAA)/AEM and covalent poly(MMA-*co*-MAA)/AEM(2) DX gel before and after immersion in pH = 7.5 buffer for 5 days. The DX hydrogel swells and is still intact in the tube (red arrow). (b) and (c) show SEM images for freeze-dried fracture surfaces of DX poly(MMA-*co*-MAA)/AEM(2) gels. (d) Frequency sweep and (e) strain sweep data for DX and SX gels. A SX gel was subjected to UV irradiation and was a control. The particle concentration used was 5 wt% and the pH was about 8.0. The legends are shared for (d) and (e).

This appeared to redisperse as aggregates; however, we have not investigated the redispersion of the SX gels in detail. It is possible that there was some pH-triggered particle fragmentation in those cases. However, the general spherical shape was maintained upon swelling as evidenced by optical microscopy of swollen particles in Fig. 1(d) and for related systems in previous work.[14,15] Importantly, the DX hydrogel did not redisperse after 5 days. Rather, the DX hydrogel swelled. It can be seen at the bottom of the vial in Fig. 3(a). This demonstrates interparticle covalent crosslinking and DX hydrogel formation. It is very likely that the shells were in contact and interpenetrated in the physically gelled state when photocrosslinking occurred. SEM images of the freeze-dried fracture surfaces of DX hydrogels (Fig. 3(b) and (c)) show similar interconnected porosity as observed for the SX gels (compare with Fig. 2(b) and (c) and also Fig. S5(b)). The interconnected porous morphology is present throughout the DX gels. The physically crosslinked morphology has been "frozen in" by the inter-shell photocrosslinking step of our new method.

Fig. 3(d) and (e) show frequency-sweep and strain-sweep dynamic rheology data for the DX hydrogel and physically crosslinked SX gels. The second AEM funtionalisation caused a major increase in G' for the physical gel compared to SX poly(MMA-*co*-MAA)/AEM gel.

(Compare the red and light blue diamonds in Fig. 3(d) and (e)). This could be due to stronger hydrophobic attractive interactions between neighbouring particles in the physically gelled state for poly(MMA-*co*-MAA)/AEM(2). Formation of the DX poly(MMA-*co*-MAA)/AEM(2) hydrogel resulted in a major increase of G' and a significant decrease of tanδ. The tanδ data are shown in Fig. S6 (ESI†). The maximum G' increased by more than 40% as a result of DX hydrogel formation. The maximum value of G' is 1040 Pa at 1 Hz for the DX hydrogel. This is a good value given the particle concentration was only 5 wt.% It is important to note that control data for the SX poly(MMA-*co*-MAA)/AEM physical gel subjected to the same UV treatment used to prepare the DX gel did not show a significant increase of G' (Fig. 3(d) and (e)) compared to the non-irradiated SX gel. This demonstrates that it was covalent-crosslinking caused by photocrosslinking that was responsible for the G' increase for the DX hydrogel. For all the systems the G' value does not significantly decrease until the strain reaches about 5%. As expected for physical gels comprising swollen particles[21] high strains cause shear-induced breakdown of the gel structure. This reduces the number density of elastically effective chains and hence G'. The DX hydrogel appears to be less ductile than the other physical gels because it had an earlier onset of the strain induced increase in tanδ (Fig. S6(b), ESI†). This is expected given that the number density of elastically effective chains has increased (and their average molecular weight has decreased) due to double crosslinking. The extent of allowable deformation of elastic chains decreases with molecular weight.

The pH-dependent swelling of the DX poly(MMA-*co*-MAA)/AEM(2) hydrogels was investigated (Fig. 4(a) and (b)). The onset swelling pH for the DX gels is much lower (*ca.* 5.8) compared to that for the SX poly(MMA-*co*-MAA)/AEM particles (Fig. 1(d)). This is about one pH unit lower than the apparent pK_a of the SX poly(MMA-*co*-MAA)/AEM(2) particles (6.9, Fig. S1†). The cause for the one pH unit decrease in the reduction in onset swelling ratio is of interest. This must originate from the differences in the starting conditions for the swelling experiments for the DX gel compared to hollow particles. The DX gel was prepared using a physically gelled state of swollen particles (Step 2, Scheme 1). The pH was subsequently decreased to measure the swelling ratios. This is opposite to the swelling experiments conducted using particles (Fig. 1(d)) where the initial state was the collapsed particles. In that case inter-segment hydrophobic interactions oppose swelling. Attractive inter-segment hydrophobic interactions are known to increase the swelling transition pH values for conventional carboxylic acid-containing hydrogels.[22] Conversely, the deswelling transition for the DX gels was not opposed in this way and is more representative of a process governed by the apparent degree of neutralisation (α) of the gel alone. For example, at a pH of 5.8 the value for α can be calculated as 0.075 using a pK_a of 6.9 and the first equation for α given in ref. 22. At this value deswelling is expected. The swelling data (Fig. 4(b)) show that near maximum swelling remained when the pH was 7.4 ($\alpha = 0.75$) for the DX hydrogels, which could be advantageous for potential regenerative medicine applications as the porosity will be maximised.

To test the hydrated DX gels for interconnected porosity we conducted a set of experiments which involved permeation of FITC-dextran (molar mass of 4000 g mol^{-1}). A FITC droplet was placed on top of an as-made DX gel, touched dry, then gel slices were removed and examined at different time periods. The method is described in the ESI and depicted in Fig. S7, ESI.† The images in Fig. 4(c) show that the FITC-dextran diffused through the gel depth (1 mm) rapidly. Complete penetration had occurred within 1 h. (In order to prevent dehydration from affecting the result different slices from the same DX gel sample are shown in Fig. 4(c).) This fast diffusion is not consistent with a honeycomb structure of intact hollow particles. Rather, it is consistent with inter-connected porosity (Fig. 3(b) and (c)). This rapid permeation should be highly advantageous for nutrient supply in future potential biomaterial applications.

Fig. 3(a) and (b) as well as 4(c) support the view that these new DX gels consist of a network of partially fragmented hollow particles. As the hollow SX particles first expand (due to the pH increase) they become trapped (caged) by neighbouring particles. Neighbouring shell segments must then come into contact and these are able to be doubly crosslinked to give permanent networks. We speculate that the interconnected porosity originates from incomplete shell formation (or shell defects) which causes (partial) shell fragmentation during pH-triggered particle swelling. We propose that shell defects originate from incomplete fusing of precipitated nanoparticles at the oil–water interface during formation of the poly(MMA-*co*-MAA) hollow particles. This rapid, high-shear, process could generate defects.

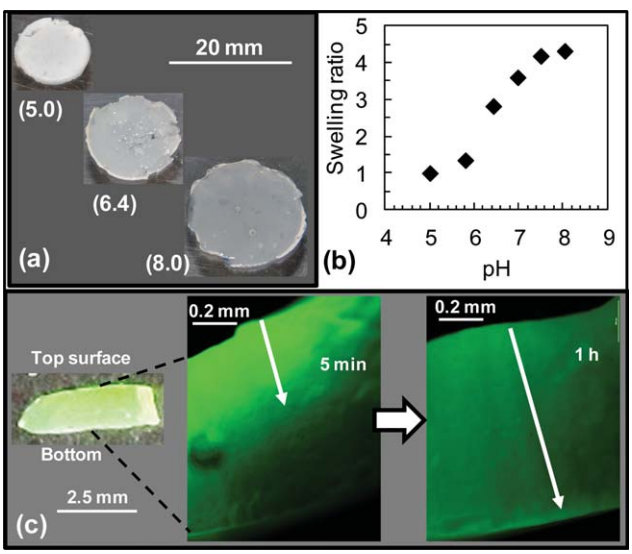

Fig. 4 pH-dependent DX hydrogel swelling and dye permeation (a) Shows digital photographs of DX poly(MMA-*co*-MAA)/AEM(2) hydrogel swollen at different pH values (shown). (b) Swelling ratio (after 7 days) as a function of pH for the DX gels. (c) shows representative fluorescence microscopy images of a hydrated DX gel (pH = 8.1) after a drop of FITC dextran solution was placed on the top surface. Complete permeation through the sample thickness occurred within 1 h. The arrow shows diffusion direction.

Conclusions

In this study we have used free-radical crosslinking of vinyl functionalised poly(MMA-*co*-MAA)/AEM hollow particles to prepare a new family of SX pH-responsive hollow particles. The SX particles form highly porous space-filling physical gels. Because they do not contain disulfides these new physical gels should be redox stable unlike earlier cystamine crosslinked systems.[15] The SX dispersions enabled preparation of a new family of pH-responsive DX hydrogels,

which were also highly porous. The DX hydrogels have a high modulus at relatively low polymer concentration. They are the first example of a covalent hydrogel prepared from pH-responsive hollow particles. The DX gels have interconnected porosity at the micrometre scale and, importantly, do not redisperse at physiological pH. They contained about 75 vol.% water at pH of about 7.4 and 0.1 M ionic strength. Because pH-responsive hollow particles are not restricted to poly(MMA-*co*-MAA)[14] the strategy demonstrated here should be generally applicable to the preparation of a range of RCOOH containing DX hydrogels. Our new method has a number of advantages. Firstly, the pK_a of the parent particles should be tuneable using particle composition[14] and this should translate to tuneability of DX gel swelling. Secondly, the average particle size of the parent particles (and hence the pore size within the DX gels) should be tuneable using the shear used to prepare the particles. Furthermore, the elasticity of the DX gel should be related to the extent of vinyl functionalisation, which is controllable. It follows that it should be possible to prepare a range of injectable, load bearing, tissue scaffolds using the new methods introduced here. Importantly, the approaches used here have not relied upon colloidal templates. Our methods are straightforward and scaleable. It is noted that poly(MMA-*co*-MAA) is structurally related to bone cement, which is a well established biomaterial. Because of these features it is likely that the new injectable hydrogels introduced here have good potential application in regenerative medicine. Work in this area is now underway at Manchester. Furthermore, the interconnected porosity and responsiveness of the DX hydrogels may enable design of high performance membranes.

Notes and references

1 E. M. Christenson, W. Soofi, J. L. Holm, N. R. Cameron and A. G. Mikos, *Biomacromolecules*, 2007, **8**, 3806.
2 O. J. Cayre and S. Biggs, *J. Mater. Chem.*, 2009, **19**, 2724.
3 C.-J. Ke, T.-Y. Su, H.-L. Chen, H.-L. Liu, W.-L. Chiang, P.-C. Chu, Y. Xia and H.-W. Sung, *Angew. Chem., Int. Ed.*, 2011, **50**, 8086.
4 A. Zelikin, Q. Li and F. Caruso, *Chem. Mater.*, 2008, **20**, 2655.
5 H. N. Yow and A. F. Routh, *Soft Matter*, 2006, **2**, 940.
6 J. Gu, F. Xia, Y. Wu, X. Qu, Z. Yang and L. Jiang, *J. Controlled Release*, 2007, **117**, 396.
7 L. Zha, Y. Zhang, W. Yang and S. Fu, *Adv. Mater.*, 2002, **14**, 1090.
8 G. Li, G. Liu, E. T. Kang, K. G. Neoh and X. Yang, *Langmuir*, 2008, **24**, 9050.
9 S. I. Ali, J. P. A. Heuts and A. M. van Herk, *Soft Matter*, 2011, **7**, 5382.
10 D. G. Shchukin and H. Mohwald, *Chem. Commun.*, 2011, **47**, 8730.
11 X. Liu, X. Jin and P. X. Ma, *Nat. Mater.*, 2011, **10**, 398.
12 I. Strehin, Z. Nahas, K. Arora, T. Nguyen and J. Elisseeff, *Biomaterials*, 2010, **31**, 2788.
13 S. A. Bencherif, D. J. Siegwart, A. Srinivasan, F. Horkay, J. O. Hollinger, N. R. Washburn and K. Matyjaszewski, *Biomaterials*, 2009, **30**, 5270.
14 R. Bird, A. J. Freemont and B. R. Saunders, *Soft Matter*, 2012, **8**, 1047.
15 R. Bird, T. J. Freemont and B. R. Saunders, *Chem. Commun.*, 2011, **47**, 1443.
16 R. Liu, A. H. Milani, T. J. Freemont and B. R. Saunders, *Soft Matter*, 2011, **7**, 4696.
17 F. Caruso, R. A. Caruso and H. Mohwald, *Science*, 1998, **282**, 1111.
18 N. Nakajima and Y. Ikada, *Bioconjugate Chem.*, 1995, **6**, 123.
19 H. H. Winter, *Polym. Eng. Sci.*, 1987, **27**, 1698.
20 H. H. Winter and F. Chambon, *J. Rheol.*, 1986, **30**, 367.
21 V. Carrier and G. Petekidis, *J. Rheol.*, 2009, **53**, 245.
22 O. E. Phippova, D. Hourdet, R. Audebert and A. R. Khokhlov, *Macromolecules*, 1997, **30**, 8278.

